Synthetic and Structural Studies on $(RC_5H_4)_4Ru_4E_4^{0/2+}$ (E = S, Se, Te): Mobile Metal–Metal Bonds within a Mixed-Valence Ru^{IV}/Ru^{III} Cluster

Eric J. Houser, Thomas B. Rauchfuss,* and Scott R. Wilson

School of Chemical Sciences, University of Illinois, 505 S. Matthews Avenue, Urbana, Illinois 61801

Received February 17, 1993

Thermolysis of solutions of $(MeC_5H_4)Ru(PPh_3)_2EH$ (E = S, Se) gives the cubane clusters $(MeC_5H_4)_4Ru_4E_4$. For the case for E = S, the coproducts were shown to be PPh_3 and H_2. A rational synthesis of PPh_4TeH is reported; this salt was employed in the preparation of $(MeC_5H_4)_4Ru_4Te_4$. This Ru_4Te_4 cluster crystallizes in the monoclinic space group $C2/c$ with a = 11.943(6) Å, b = 18.623(6) Å, c = 12.590(7) Å, V = 2792(4) Å^3, and Z = 8. Structural trends show that the identity of the chalcogen more strongly affects the nonbonding Ru···Ru, Ru···E, and E···E interactions than the bonding interactions. The clusters undergo 2e oxidations as demonstrated by cyclic voltammetry studies. Chemical oxidations using $(MeC_5H_4)_2Fe^+$ gave salts of the dications $(MeC_5H_4)_4Ru_4E_4^{2+}$ (E = S, Se, Te). The dicationic S_4 and Se_4 clusters exhibit dynamic ^1H NMR properties such that at low temperatures signals for two $CH_3C_5H_4$ groups were observed while at high temperatures the MeC_5H_4 groups appear equivalent. On the basis of coalescence temperatures, the barriers were estimated as ~52 kJ/mol. In a test of the possible influence of steric factors on the dynamics, the DNMR properties of the new derivative $(Me_3SiC_5H_4)_4Ru_4S_4(PF_6)_2$ were shown also to be very similar to the MeC_5H_4 clusters. The $Me_3SiC_5H_4$ cluster crystallizes in the monoclinic space group $P2_1/c$ with a = 18.828(2) Å, b = 12.421(1) Å, c = 21.451(1) Å, β = 92.442(1)°, V = 5012 Å^3, and Z = 4. The structure confirms the presence of three Ru–Ru bonding distances. Variable-temperature NMR experiments on $(MeC_5H_4)_4Fe_4S_4^{2+}$ and $(MeC_5H_4)_4Ru_4S_4$ gave no evidence of structural dynamics.

Introduction

In contrast to the situation for bulk metals, many low-dimensional and molecular species feature localized metal–metal interactions. The existence of such localized metal–metal interactions has prompted numerous investigations of their structure and stereochemistry. Less studied are the *dynamics* of metal–metal bonds. Progress on this theme is surveyed in the following paragraphs, beginning with cases of metal–metal bond/no bond equilibria.

The phenomenon of a metal–metal bond/no bond equilibrium is illustrated by $Cp_2Cr_2(CO)_6$, which spontaneously homolyzes in solution to give the 17e species $CpCr(CO)_3$ (eq 1). The fragility

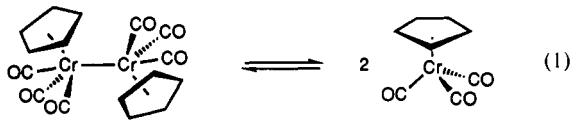

(1)

of $Cp_2Cr_2(CO)_6$ is indicated by the long Cr–Cr bond length of 3.281 Å, which arises because of steric crowding.[1,2] An intramolecular example of metal–metal bond/no bond equilibria was recently proposed by Kölle[3] to account for the temperature dependence of the ^1H NMR spectrum of $(C_5R_5)_2Ru_2X_4$, where X = Cl, Br. These workers crystallized two forms of the dimer which differ with respect to their Ru–Ru distances (eq 2). Related

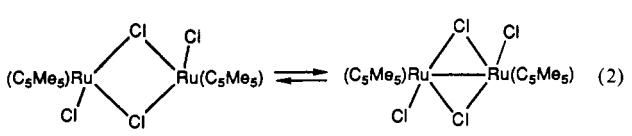

(2)

singlet–triplet equilibria have been observed for 50e$^-$ $(C_5R_5)_3Co_3S_2$ and 46e$^-$ $(C_5R_5)_3Co_3(CO)_2$.[4] Evidence for metal–metal bond cleavage involving *multinuclear* fragments has been presented by Heaton, who employed ^{195}Pt NMR spectroscopy to demonstrate site exchange between $Pt_{12}(CO)_{24}^{2-}$ and $Pt_9(CO)_{18}^{2-}$ (eq 3).[5] Other examples of reversible intramolecular metal–

$$Pt^*_{12}(CO)_{24}^{2-} + Pt_9(CO)_{18}^{2-} \rightleftharpoons Pt^*_9(CO)_{18}^{2-} + Pt_{12}(CO)_{24}^{2-} \quad (3)$$

metal bond cleavage are depicted in Scheme I.[6–8]

The tetranuclear cluster $W_4(O^iPr)_{12}$ exhibits dynamic behavior as indicated by NMR line broadening and magnetization transfer experiments. To account for these NMR measurements, Chisholm and co-workers invoke a metallacyclobutadiene-like intermediate which interchanges W–W bonding contacts of 2.50 and 2.73 Å (eq 4, R = ^{i}Pr).[9]

Highly relevant to our work are the dynamics of cubane clusters $Cp_4Fe_4S_5^z$ (z = 0, 2+) and the MeC_5H_4 analogues.[10,11] These clusters are derivatives of $Cp_4Fe_4S_4$ by replacement of one μ_3-S

(1) Adams, R. D.; Collins, D. E.; Cotton, F. A. *J. Am. Chem. Soc.* **1974**, *96*, 749.
(2) Leading reference: Hoobler, R. J.; Hutton, M. A.; Dillard, M. M.; Castellani, M. P.; Rheingold, A. L.; Rieger, A. L.; Rieger, P. H.; Richards, T. C.; Geiger, W. E. *Organometallics* **1993**, *12*, 116.
(3) Kölle, U.; Kossakowski, J.; Klaff, N.; Wesemann, L.; Englert, U.; Heberich, G. E. *Angew. Chem., Int. Ed. Engl.* **1991**, *30*, 690; *Angew. Chem.* **1991**, *103*, 732.
(4) Sorai, M.; Kosaki, A.; Suga, H.; Seki, S.; Yoshida, T.; Otsuka, S. *Bull. Chem. Soc. Jap.* **1971**, *44*, 2364. Pulliam, C. R.; Thoden, J. B.; Stacy, A. M.; Spencer, B.; Englert, M. H.; Dahl, L. F. *J. Am. Chem. Soc.* **1991**, *113*, 7398. Barnes, C. E.; Dial, M. R.; Orvis, J. A.; Staely, D. L.; Rheingold, A. L. *Organometallics* **1990**, *9*, 1021 and references therein.
(5) Brown, C.; Heaton, B. T.; Chini, P.; Fumagalli, A.; Longoni, G. *J. Chem. Soc., Chem. Commun.* **1977**, 309.
(6) Carmona, D.; Ferrer, J.; Mendoza, A.; Lahoz, F. J.; Reyes, J.; Oro, L. A. *Angew. Chem., Int. Ed. Engl.* **1991**, *30*, 1171; *Angew. Chem.* **1991**, *103*, 1192.
(7) Jones, R. A.; Wright, T. C.; Atwood, J. L.; Hunter, W. E. *Organometallics* **1983**, *2*, 470.
(8) Bailey, D. A.; Balch, A. L.; Fossett, A.; Olmstead, M. M.; Reedy, P. E., Jr. *Inorg. Chem.* **1987**, *26*, 2413.
(9) Chisholm, M. H.; Clark, D. L.; Hampden-Smith, M. J. *J. Am. Chem. Soc.* **1989**, *111*, 574.
(10) Kubas, G. J.; Vergamini, P. J. *Inorg. Chem.* **1981**, *20*, 2667.
(11) Blonk, H. L.; Mesman, J.; van der Linden, J. G. M.; Steggerda, J. J.; Smits, J. M. M.; Beurskens, G.; Beurskens, P. T.; Tonon, C.; Jordanov, J. *Inorg. Chem.* **1992**, *31*, 962. Blonk, H. L.; van der Linden, J. G. M.; Steggerda, J. J.; Jordanov, J. *Inorg. Chim. Acta* **1989**, *158*, 239. Other examples of localized bonding in Fe_4S_5 clusters are described in: Inomata, S.; Tobita, H.; Ogino, H. *Inorg. Chem.* **1992**, *31*, 722.

0020-1669/93/1332-4069$04.00/0

Scheme I

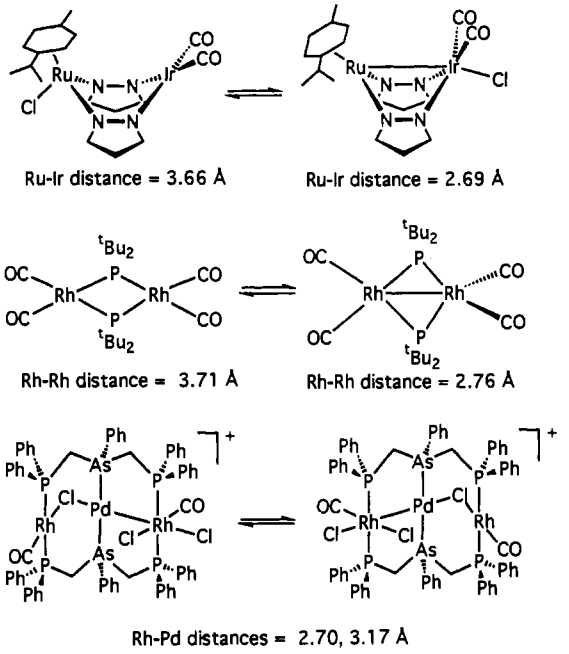

by μ_3-S_2. ^{1}H NMR studies on $Cp_4Fe_4S_5$ show a 1:2:1 pattern of Cp resonances which collapses at higher temperatures to a 1:3 pattern indicating that Fe–Fe bonds migrate in step with rotation of the S_2 group (eq 5). Comparable dynamics occur in $Cp_4Fe_4S_5^{2+}$

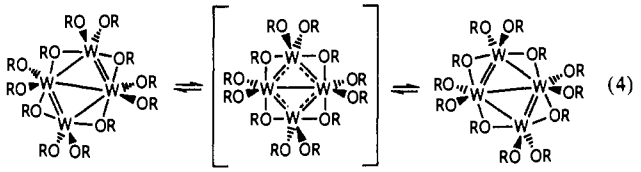

(4)

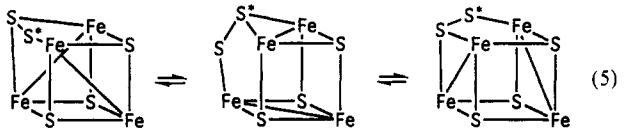

(5)

but at higher temperatures.

As illustrated in the examples above, when ligand dynamics modify the electron count of a metal center within a cluster, one expects to observe correlated changes in the metal–metal bonding. Conceptually distinct are those examples where dynamics result from redox events within the cluster.[4] This effect is more prevalent for odd-electron ensembles where the structural consequences are often sufficiently subtle that the dynamics can even be observed in the solid state.[12] In this paper we provide details[13] of cluster dynamics resulting from internal redox with the following characteristics: (i) The species are diamagnetic, (ii) the redox events result in substantial structural changes at the affected metals, and (iii) the clusters have been examined under both fast- and slow-exchange limits.

Results

Synthesis of Ru_4E_4 Cubane Clusters. The Ru_4E_4 (E = S, Se) clusters are prepared simply by heating toluene solutions of $(MeC_5H_4)Ru(PPh_3)_2EH$.[14] The corresponding Cp clusters are virtually insoluble in common organic solvents. In the synthesis of $(MeC_5H_4)_4Ru_4S_4$ we showed that the coproducts are PPh_3 and H_2.[15] The yield of hydrogen was quantified by conducting the thermolysis reaction in a closed system (eq 6). We also prepared $(Me_3SiC_5H_4)_4Ru_4S_4$ via the same method, starting with $(Me_3SiC_5H_4)Ru(PPh_3)_2SH$. The $Me_3SiC_5H_4$ cluster proved to be extremely soluble in organic solvents.

$$4(RC_5H_4)Ru(PPh_3)_2EH \rightarrow (RC_5H_4)_4Ru_4E_4 + 2H_2 + 8PPh_3 \quad (6)$$

$$R = H, Me; E = S, Se, Te$$

The preparation of $(MeC_5H_4)_4Ru_4Te_4$ was modeled after the corresponding sulfide and selenide clusters, although we did not establish the intermediacy of $(MeC_5H_4)Ru(PPh_3)_2TeH$. The Ru_4Te_4 and Ru_4Se_4 clusters were characterized by ^{125}Te and ^{77}Se NMR, which showed a single line. As a tellurium source, we used $(PPh_4)TeH$, whose structure and serendipitous isolation has been described by Haushalter.[16] This salt can be prepared in good yield by the addition of PPh_4Cl to a partially acidified aqueous solution of Na_2Te. Orange crystals of $(PPh_4)TeH$ are slightly light-sensitive and highly air-sensitive. The salt is readily soluble in polar organic solvents such as acetonitrile, methanol, and DMF. Its solubility characteristics parallel those of PPh_4I, with which it is isostructural. The ^{1}H NMR chemical shift for the Te*H* is −13.4 ppm.

The neutral cubane clusters were doubly oxidized using 2 equiv of $(MeC_5H_4)_2FePF_6$ (eq 7, cyclopentadienyl groups omitted).

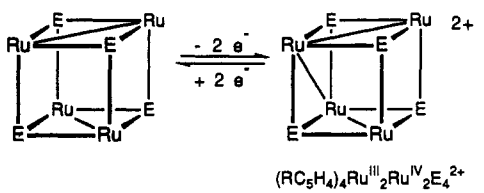

(7)

$(RC_5H_4)_4Ru^{III}_2Ru^{IV}_2E_4^{2+}$

The choice of this oxidant was guided by electrochemical data for the clusters (see below) as well as the high solubility of $(MeC_5H_4)_2Fe$, which facilitates its separation from the ionic products. The dicationic clusters proved to be moderately air stable and were characterized by elemental analyses, mass spectrometry, and ^{1}H NMR spectroscopy. The structure of the tetracyanoquinodimethanide, $(TCNQ)_2^{2-}$, salt of $(MeC_5H_4)_4Ru_4S_4^{2+}$ has been reported by us previously;[13] this paper presents structural details on the diamagnetic $(Me_3SiC_5H_4)_4Ru_4S_4(PF_6)_2$.

Structure of $(MeC_5H_4)_4Ru_4Te_4$. The structure of $(MeC_5H_4)_4Ru_4Te_4$ can be viewed as a nested dimer of $(MeC_5H_4)_2Ru_2Te_2$ butterfly subunits each of which features a single Ru–Ru bond and two bridging tellurium atoms (Figure 1). The two bonding Ru–Ru distances average 2.89 Å; the four nonbonding Ru···Ru distances average 4.02 Å. The metal–metal bonded distance may be compared to 2.76 Å for the Ru_4S_4 analogue.[17] The nonbonded Ru···Ru contacts are 0.42 Å longer than in the Ru_4S_4 cluster, reflecting the greater size of Te vs S. The average intrabutterfly Te···Te distance is 3.92 Å, while the average interbutterfly Te···Te distance is 3.27 Å. Intercluster Te···Te contacts of ~4.49 Å are

(12) Leading references to this active area: Jang, Ho G.; Geib, S. J.; Kaneko, Y.; Nakano, M.; Sorai, M.; Rheingold, A. L.; Montez, B.; Hendrickson, D. N. *J. Am. Chem. Soc.* **1989**, *111*, 173.

(13) Preliminary account: Houser, E. J.; Amarasekera, J.; Rauchfuss, T. B.; Wilson, S. R. *J. Am. Chem. Soc.* **1991**, *113*, 7441.

(14) Amarasekera, J.; Rauchfuss, T. B. *Inorg. Chem.* **1989**, *28*, 3875. Amarasekera, J.; Houser, E. J.; Rauchfuss, T. B.; Wilson, S. R. *Inorg. Chem.* **1992**, *31*, 1614. Amarasekera, J. Ph.D. Thesis, University of Illinois, Urbana, IL, 1988.

(15) Other examples of complexes that remove H_2 from H_2S: Besenyei, G.; Lee, C.-L.; Gulinski, J.; Rettig, S. J.; James, B. R.; Nelson, D. A.; Lilga, M. A. *Inorg. Chem.* **1987**, *26*, 3622. Rabinovich, D.; Parkin, G. *J. Am. Chem. Soc.* **1991**, *113*, 5904.

(16) Huffman, J. C.; Haushalter, R. C. *Polyhedron* **1987**, *8*, 531. Björgvinsson, M.; Schrobilgen, G. J. *Inorg. Chem.* **1991**, *30*, 2540.

(17) $(MeC_5H_4)_4Ru_4S_4$ and $(MeC_5H_4)_4Ru_4Se_4$: Amarasekera, J.; Rauchfuss, T. B.; Wilson, S. R. *J. Chem. Soc., Chem. Commun.* **1989**, 14.

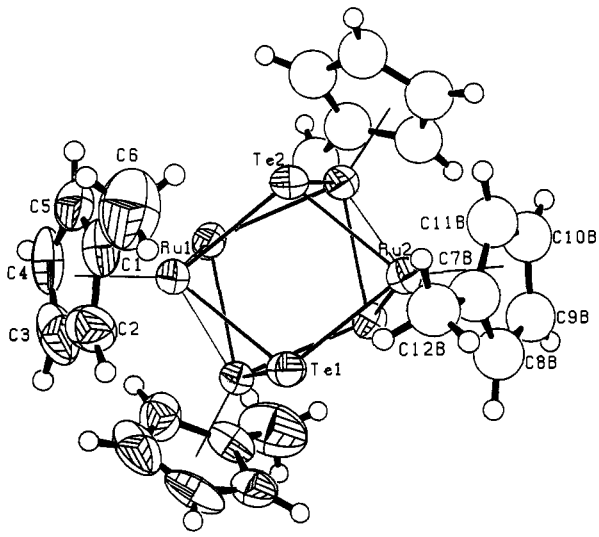

Figure 1. Structure of $(MeC_5H_4)_4Ru_4Te_4$ with thermal ellipsoids drawn at the 35% probability level.

Table I. Average Distances (Å) and Angles (deg) for $(MeC_5H_4)_4Ru_4E_4$ (E = S, Te)[a]

param	$(MeC_5H_4)_4Ru_4S_4$[d]	$(MeC_5H_4)_4Ru_4Te_4$
Ru–Ru[b]	2.76	2.89
Ru···Ru[c]	3.60	4.02
Ru–Cp (centroid)	1.87	1.88
Ru–E[b]	2.31	2.59
Ru–E[c]	2.37	2.65
E···E[c]	2.96	3.27
E···E[b]	3.45	3.92
Ru–E–Ru[b]	73.3	67.9
Ru–E–Ru[c]	100.9	100.5
E–Ru–E[b]	96.4	98.7
E–Ru–E[c]	77.8	77.4

[a] Esd's are not included; these are average distances with small esd's. [b] Parameters for $(MeC_5H_4)_2Ru_2E_2$ "butterfly" subunits wherein the two Ru atoms are mutually bonded. [c] Parameters for $(MeC_5H_4)_2Ru_2E_2$ rhombs which feature nonbonded Ru···Ru contacts. [d] From ref 9.

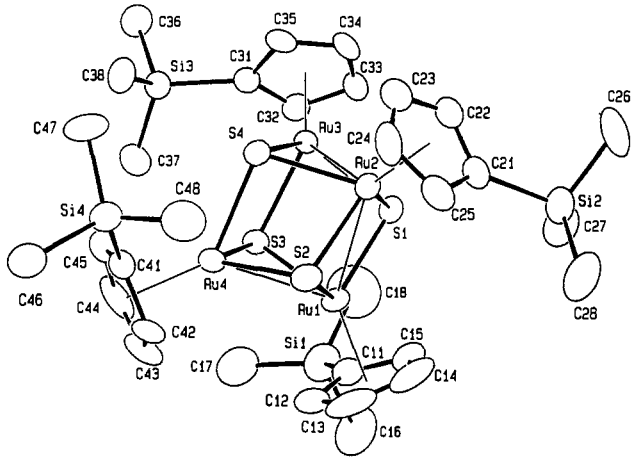

Figure 2. Structure of the dication in $(Me_3SiC_5H_4)_4Ru_4S_4(PF_6)_2$ with thermal ellipsoids drawn at the 35% probability level.

presumed to be unimportant. The structural parameters for $(MeC_5H_4)_4Ru_4Te_4$ are presented in Table I along with those for $(MeC_5H_4)_4Ru_4S_4$.

Structure of $(Me_3SiC_5H_4)_4Ru_4S_4(PF_6)_2$. The dication was found to be similar to that found in $(MeC_5H_4)_4Ru_4S_4(TCNQ)_2$, as described in a preliminary communication.[13] The cubane core is distorted from idealized T_d symmetry by virtue of three Ru–Ru bonds and three Ru···Ru nonbonding distances averaging 2.80 and 3.53 Å, respectively (Figure 2). The corresponding distances in $(MeC_5H_4)_4Ru_4S_4(TCNQ)_2$ are 2.79 and 3.50 Å. The Ru–S

Table II. Distances (Å) and Angles (deg) for $(Me_3SiC_5H_4)_4Ru_4S_4(PF_6)_2$ and $(MeC_5H_4)_4Ru_4S_4(TCNQ)_2$

param	$(Me_3SiC_5H_4)_4$-$Ru_4S_4(PF_6)_2$[a]	$(MeC_5H_4)_4$-$Ru_4S_4(TCNQ)_2$[b]
Ru–Ru	2.807, 2.797, 2.800(1)	2.7848, 2.7937, 2.7836(6)
Ru···Ru	3.53	3.50
Ru–S	2.31	2.31
Ru–RCp(centroid)	1.88	1.87
S···S	3.25	3.26
Ru–S–Ru[c]	75.1	74.8
Ru–S–Ru[d]	98.3	97.7
S–RuS[c]	102.0	102.5
S–Ru–S[d]	77.7	78.1

[a] Except for the close Ru–Ru contacts, the angles and distances are averages. Esd's are not included as they are small compared to the averaged values. [b] Reference 13. TCNQ is tetracyanoquinodimethanide. [c] Angles which occur on a Ru–Ru bonded cluster face. [d] Angles which occur on a Ru···Ru nonbonded cluster face.

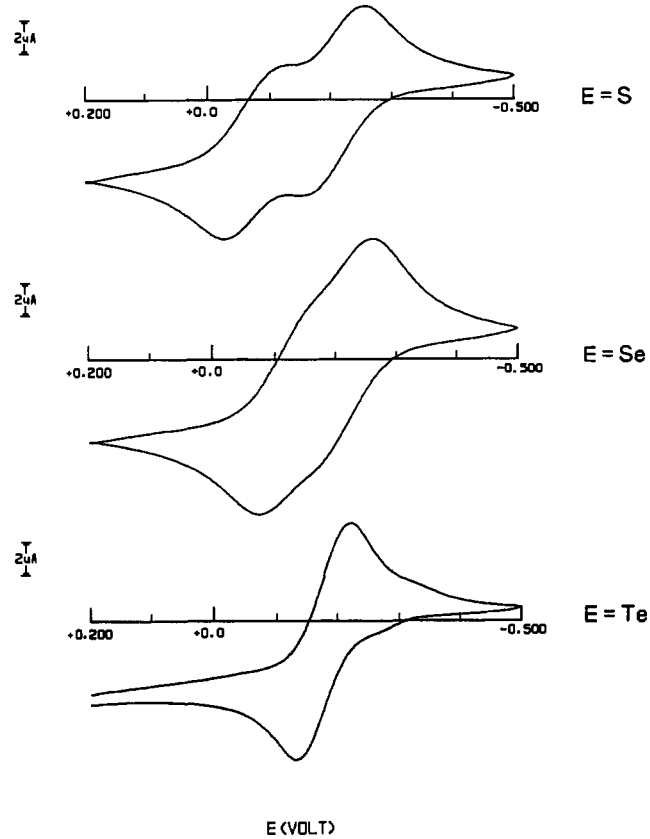

Figure 3. Cyclic voltammograms of $(MeC_5H_4)_4Ru_4E_4$ (E = S, Se, Te). See Table III for details.

distances in $(Me_3SiC_5H_4)_4Ru_4S_4^{2+}$ range 2.267(3)–2.375(2) Å with an average Ru–S distance of 2.31 Å, the same as in $(MeC_5H_4)_4Ru_4S_4(TCNQ)_2$. For $(Me_3SiC_5H_4)_4Ru_4S_4^{2+}$, the Ru–S–Ru and S–Ru–S angles on Ru–Ru bonded cluster faces average 75.1 and 102.0°, while those on the faces lacking Ru–Ru bonds are 98.3 and 77.7°. These parameters are within 2° of those in $(MeC_5H_4)_4Ru_4S_4^{2+}$ (Table II).

Electrochemistry. The cyclic voltammograms of the MeC_5H_4-containing clusters were recorded under identical conditions (Figure 3). We observed that the average of the two oxidation potentials $(E_{1/2})_{av}$ varied by only ~30 mV upon changing from S to Se to Te (Table III). The chalcogen exerts a more profound effect on $\Delta E_{1/2}$, the difference between the first and second oxidation waves. For E = S two distinct processes can be observed with $\Delta E_{1/2} \approx 121$ mV, while for E = Te only a single electrochemical event is observed with $\Delta E_p = 94$ mV.

Cyclic voltammetry measurements were also conducted on salts of the doubly oxidized clusters. These cyclic voltammograms

Table III. $E_{1/2}$ Values (mV) for $(Me_3SiC_5H_4)_4Ru_4S_4$ and $(MeC_5H_4)_4Ru_4E_4$

RC_5H_4	E	$E_{1/2}$[a]	$(E_{1/2})_{av}$	$\Delta E_{1/2} = (E_{1/2})_1 - (E_{1/2})_2$
MeC_5H_4	S	−62/−183	−123	121
MeC_5H_4	Se	−94/−175	−134	~80
MeC_5H_4	Te	−170	−170[b]	0
$Me_3SiC_5H_4$	S	+30/−140	−55	170

[a] All data vs Ag/AgCl reference electrode with 0.1 M Bu_4NPF_6, Pt electrodes, and CH_2Cl_2 solutions; the scan rates were 100 mV/s. [b] ΔE_p = 94 mV, where $\Delta E_p = E_{pc} - E_{pa}$ and E_{pc} is the peak potential for the cathodic wave and E_{pa} is the peak potential for the anodic wave.

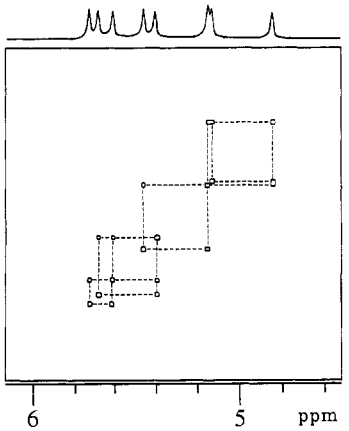

Figure 4. ^1H–^1H Correlation spectrum (500 MHz) for $(MeC_5H_4)_4Ru_4S_4(PF_6)_2$ at −43 °C, CD_3CN solution.

are similar to those of the parent neutral complexes except that we were unable to resolve the two waves for the $Ru_4S_4^{2+}$ case. Nonetheless, the overall patterns confirm that these clusters are indeed undergoing 2e⁻ processes. Further evidence for 2e⁻ transfer is provided by the values for ΔE_p, the difference in the peak potentials for cathodic and anodic waves. These values are 84 (S), 46 (Se), and 41 mV (Te). The theoretical value of ΔE_p for a reversible 2e⁻ couple is 29 mV.[18]

Dynamic NMR Studies. The ^1H NMR spectrum of $(MeC_5H_4)_4Ru_4S_4^{2+}$ was found to be temperature dependent such that at low temperatures (below ~−30 °C) two nonequivalent MeC_5H_4 ligands were observed. This behavior is seen both for the methyl singlets and the MeC_5H_4 backbone signals. The coalescence temperature (T_c = −8 °C) for the methyl singlets indicates a free energy barrier (ΔG^*) of 52 kJ/mol on the basis of the coalescence temperature.[19] The coalescence temperature was unaffected by a 10-fold change in concentration of $(MeC_5H_4)_4Ru_4S_4(PF_6)_2$, indicating that the observed dynamics are *intramolecular*.

Stereochemical insight into the process was provided by the details of the MeC_5H_4 signals. At high temperatures (20 °C) only two MeC_5H_4 signals were observed indicative of only two MeC_5H_4 backbone sites, while at the low-temperature limit (−43 °C) eight MeC_5H_4 signals were observed. As seen in Figures 4 and 5, we do not resolve the individual H–H coupling constants although the widths of the MeC_5H_4 peaks at half-height are noticeably broad (8 Hz) vs the 1.8-Hz width for the CH_3 peaks. The connectivity of these MeC_5H_4 signals in the slow-exchange limit can be deduced by a 2-dimensional ^1H–^1H *J*-correlation experiment (COSY), conducted at −43 °C (Figure 4). It is evident

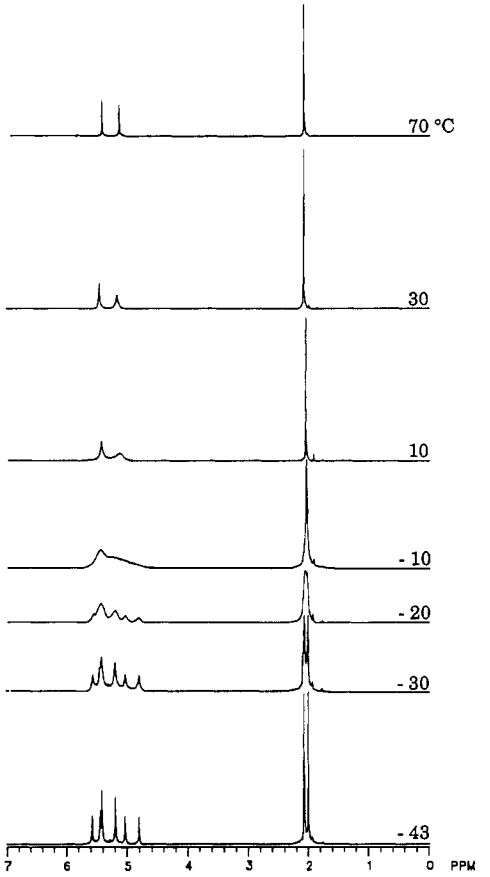

Figure 5. Variable-temperature 500-MHz ^1H NMR spectra of CD_3CN solution of $(MeC_5H_4)_4Ru_4Se_4(PF_6)_2$.

Table IV. Free Energy Barriers (ΔG^*) for Dynamics in $(RC_5H_4)_4Ru_4E_4^{2+}$ Clusters (E = S, Se, Te) from ^1H NMR Peak Coalescence

RC_5H_4	E	T_c (°C)	ΔG^* (kJ/mol)
MeC_5H_4	S	−8	52(±1)[a,b]
MeC_5H_4	Se	−21	52(±1)[a,c]
MeC_5H_4	Te		<50[b] (±1)[a]
$Me_3SiC_5H_4$	S	−8	55(±1)[d]

[a] CD_3CN solution. [b] The following activation parameters were determined from line shape analysis: ΔG^*(265 K) = 52(2) kJ/mol, ΔH^* = 39(2) kJ/mol, ΔS^* = −51(4) J/K mol. [c] The following activation parameters were determined from line shape analysis: ΔG^*(252 K) = 52(2) kJ/mol, ΔH^* = 45(2) kJ/mol, ΔS^* = −27(4) J/K mol. [d] $(CD_3)_2CO$ solution.

from the COSY data that the MeC_5H_4 signals arise from two independent ABCD spin systems indicating a pair of magnetically nonequivalent MeC_5H_4 groups. Further analysis of the COSY data reveals that the two signals of each ABCD set correlate with only one other signal indicating that these signals arise from the protons flanking the methyl group (A and D sites) on the MeC_5H_4. Similarly the two other signals of each ABCD subset display *two* cross peaks indicating that they arise from protons which are coupled to two other sites. These low-temperature results are consistent with the X-ray structure determinations of $(Me_3SiC_5H_4)_4Ru_4S_4(PF_6)_2$ and $(MeC_5H_4)_4Ru_4S_4(TCNQ)_2$,[13] which reveal cluster dications of idealized C_2 symmetry.

We considered the possibility that the observed dynamics arise from hindered rotation about the MeC_5H_4–Ru axis, caused by interactions between adjacent MeC_5H_4 groups. This posibility is excluded by the DNMR properties of $(Me_3SiC_5H_4)_4Ru_4S_4(PF_6)_2$, where the free energy barrier (ΔG^*), determined from T_c for the $(CH_3)_3Si$ signals, was 56 kJ/mol, only ~3 kJ/mol more than the MeC_5H_4 analogue (Table IV). Also consistent with the relative unimportance of hindered rotation in these cubane

(18) Leading references to 2e⁻ redox processes in M–M bonded clusters: Tolyathan, B.; Geiger, W. E. *J. Am. Chem. Soc.* **1985**, *107*, 5960. Bedard, R. L.; Dahl, L. F. *J. Am. Chem. Soc.* **1986**, *108*, 5933. Boyer, W. J.; Merkert, J. W.; Geiger, W. E. *Organometallics* **1989**, *8*, 191. Pierce, D. T.; Geiger, W. E. *J. Am. Chem. Soc.* **1989**, *111*, 7636. Finke, R. G.; Voegeli, R. H.; Laganis, E. D.; Boekelheide, V. *Organometallics* **1983**, *2*, 347. Lockemeyer, J. R.; Rauchfuss, T. B.; Rheingold, A. L. *J. Am. Chem. Soc.* **1989**, *111*, 5733. Koide, Y.; Bautista, M. T.; White, P. S.; Schauer, C. K. *Inorg. Chem.* **1992**, *31*, 3690.

(19) Friebolin, H. *Basic One- and Two-Dimensional NMR Spectroscopy*; VCH: Weinheim, Germany, 1991.

clusters is the absence of temperature effects on the ^1H NMR spectrum of $(MeC_5H_4)_4Ru_4S_4$.

The ambient-temperature ^1H NMR spectra of both $(MeC_5H_4)_4Ru_4E_4(PF_6)_2$ (E = Se, Te) complexes are similar to that seen for $(MeC_5H_4)_4Ru_4S_4^{2+}$. The low-temperature (−43 °C) spectrum for $(MeC_5H_4)_4Ru_4Se_4^{2+}$ shows two CH_3 resonances and six signals for the MeC_5H_4 region with relative intensities of 1:1:2:2:1:1 (Figure 5). The T_c of −21 °C indicates a ΔG^* value of 52 kJ/mol. The −40 °C ^1H NMR spectrum of $(MeC_5H_4)_4Ru_4Te_4^{2+}$ showed only slight broadening. Assuming that $\Delta\delta_{Me}$ is similar for Te and Se, a free energy barrier of ≤50 kJ/mol would be indicated for $(MeC_5H_4)_4Ru_4Te_4^{2+}$.

The energetics associated with the structural dynamics of $(MeC_5H_4)_4Ru_4S_4^{2+}$ (E = S, Se) were also evaluated by computer simulation of the CH_3 signals at several temperatures (Table IV). The values of ΔG^* calculated in this way compare favorably with those calculated on the basis of T_c alone. The temperature dependence of the rates shows that, at the temperatures of interest, the barrier is primarily enthalpic. ΔH^* for the Se_4 cluster is somewhat larger than that for the analogous $(MeC_5H_4)_4Ru_4S_4^{2+}$.

The ^1H NMR spectrum of $(MeC_5H_4)_4Fe_4S_4(PF_6)_2$ showed no evidence for structural dynamics over the range −40 to 25 °C. This is consistent with the solid-state structure of $(C_5H_5)_4Fe_4S_4^{2+}$, whose core is of approximate D_{2d} symmetry with four short Fe–Fe contacts assigned bond orders of $^3/_4$.[20] This result also indicates that steric effects are not responsible for the DNMR results.

Discussion

Efficient syntheses have been developed for the series $(MeC_5H_4)_4Ru_4E_4$, where E = S, Se, and Te. The preparative routes rely on the ready availability of $(RC_5H_4)Ru(PPh_3)_2Cl$ and new sources of SeH^- and TeH^-. In the case of E = S and Se, $(MeC_5H_4)Ru(PPh_3)_2EH$ are demonstrated intermediates.[14] Our unsuccessful effort to isolate $(MeC_5H_4)Ru(PPh_3)_2TeH$ is not surprising as tellurols are often unstable[21] in the absence of imposing steric effects. The liberation of triphenylphosphine is observed in these preparations, and in the case of the MeC_5H_4–Ru–S system, the evolution of hydrogen was demonstrated. The formation of hydrogen is suggestive of the intermediate compound containing pairs of RuSH centers, e.g., $[(C_5H_5)Ru(PPh_3)(\mu\text{-}SH)]_2$, whereby the hydrogen atoms can combine intramolecularly. Relevant to this point is Shaver's observation that $(C_5H_5)Ru(PPh_3)_2SR$ (R = alkyl) thermally condenses to give $[(C_5H_5)Ru(PPh_3)(\mu\text{-}SR)]_2$ followed by formation of $[(C_5H_5)Ru(\mu\text{-}SR)]_3$.[22]

Homometallic $(RC_5H_4)_4M_4S_4$ clusters are well-known for the first transition series.[23,24] The only prior studies on second-row derivatives had focused on $(RC_5H_4)_4Mo_4E_4$ (E = S, Se)[25] and $(C_5Me_5)_4M_4S_4$ (M_4 = Rh_4, Rh_2Ir_2, Ir_4).[26] The kinetic stability and diverse redox chemistry renders these clusters attractive building blocks for future endeavors. As we highlight in this work, an added feature of these compounds is the stereochemical perturbation associated with localized M–M bonds.

Given our emphasis on mobile metal–metal bonds in $(MeC_5H_4)_4Ru_4E_4^{2+}$, it is relevant to review the structural evidence

Chart I

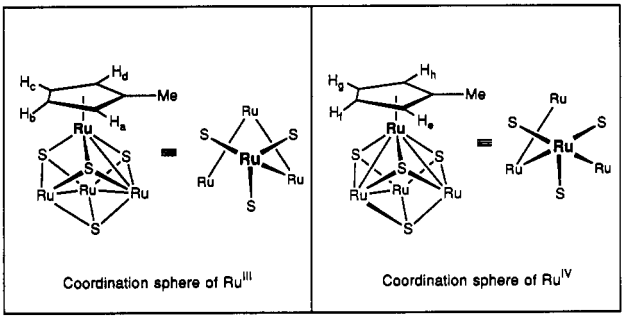

supporting localized Ru–Ru bonding in these clusters. First, the so-called Ru–Ru bonding distances are short and span a narrow range from 2.74 to 2.81 Å. The Ru–Ru bond in hcp Ru metal is 2.68 Å.[27] If one assigns η^5-C_5R_5 as a tridentate ligand, the coordination number for the Ru centers in these clusters could be described as 7 or 8, depending on the number of Ru–Ru bonds. Consistent with Ru–Ru bonding in $(MeC_5H_4)_4Ru_4S_4^{2+}$, there are three Ru–Ru contacts which are of equal length and within 2% of those for the neutral precursors. Last, Ru–Ru bonding is supported by the effects of the chalcogen size on the intracluster distances. Changing from S to Te more strongly influences nonbonding distances than bonding ones. For example, in the MeC_5H_4-containing clusters the nonbonding Ru···Ru distances increase by 0.42 Å on changing from S to Te, while the bonding Ru–Ru distance increased by only 0.13 Å. The fact that the bonding Ru–Ru contacts respond at all to the Te for S change is in accord with electronic structure calculations, which indicate that the highest energy bonding molecular orbitals are M–M bonding.[23] The low symmetry of the Ru_4S_4 cluster cores in $(Me_3SiC_5H_4)_4Ru_4S_4(PF_6)_2$ and $(MeC_5H_4)_4Ru_4S_4(TCNQ)_2$ invites assignment of localized oxidation states to the ruthenium centers as pairs of Ru^{IV} and Ru^{III} sites with the Ru^{IV} sites being associated with two Ru–Ru bonds (Chart I). From this perspective, the dynamics involve intramolecular electron transfer.

The most noteworthy feature of the electrochemical results is the closeness of the potentials for the two oxidation waves. Such small $\Delta E_{1/2}$ values are often associated with redox process coupled

(20) Trinh-Toan; Teo, B. K.; Ferguson, J. A.; Meyer, T. J.; Dahl, L. F. *J. Am. Chem. Soc.* **1977**, *99*, 408.

(21) A rare example of a terminal tellurol complex is $[M(CO)_5TeH]^-$ (M = Cr, Mo): Hausmann, H.; Höfler, M.; Kruck, T.; Zimmerman, H. W. *Chem. Ber.* **1981**, *114*, 975. Recent results on TeH compounds: Dabbousi, B. O.; Bonasia, P. J.; Arnold, J. *J. Am. Chem. Soc.* **1991**, *113*, 3186. Bochmann, M.; Coleman, A. P.; Webb, K. J.; Hursthouse, M. B.; Mazid, M. *Angew. Chem., Int. Ed. Engl.* **1991**, *30*, 973; *Angew. Chem.* **1991**, 975. For an overview of tellurol chemistry see: Rauchfuss, T. B. In *The Chemistry of Organic Selenium and Tellurium Compounds*; Patai, S., Ed.; J. Wiley: New York, 1987; Vol. 2, p 339.

(22) Shaver, A.; Plouffe, P.-Y.; Liles, D. C.; Singleton, E. *Inorg. Chem.* **1992**, *31*, 997.

(23) Harris, S. *Polyhedron* **1989**, *8*, 2843. Kharas, K. C. C.; Dahl, L. F. *Adv. Chem. Phys.* **1988**, *70*, 1.

(24) Representative papers are listed by metal core. $(MeC_5H_4)_4Ti_4S_4$: Darkwa, J.; Lockemeyer, J. R.; Boyd, P. D. W.; Rauchfuss, T. B.; Rheingold, A. L. *J. Am. Chem. Soc.* **1988**, *110*, 141. $(C_5R_5)_4V_4S_4$: Bolinger, C. M.; Darkwa, J.; Gammie, G.; Gammon, S. E.; Lyding, J. W.; Rauchfuss, T. B.; Wilson, S. R. *Organometallics* **1986**, *5*, 2386. Pasynskii, A. A.; Eremenko, J. L.; Katugin, A. S.; Gasanov, G. Sh.; Turchanova, E. A.; Ellert, O. G.; Struchkov, Yu T.; Shklover, V. E.; Berberova, N. T.; Sogomonova, A. G.; Okhlobystin, O. Yu *J. Organomet. Chem.* **1988**, *344*, 195. Herberhold, M.; Schrepfermann, M.; Darkwa, J. *J. Organomet. Chem.* **1992**, *430*, 61. $(C_5R_5)_4Cr_4S_4$: Pasynskii, A. A.; Eremenko, I. L.; Rakitin, Yu. V.; Novotortsev, V. M.; Ellert, O. G.; Kalminnikov, V. T.; Shklover, V. E.; Struchkov, Yu. T.; Lindeman, S. V.; Kurbanov, T. Kh.; Gasanov, G. Sh. *J. Organomet. Chem.* **1983**, *248*, 309. Eremenko, I. L.; Nefedov, S. E.; Pasynskii, A. A.; Orazsakhatov, B.; Ellert, O. G.; Struchkov, Yu. T.; Yanovsky, A. I.; Zagorevsky, D. V. *J. Organomet. Chem.* **1989**, *368*, 185. $Cp_4Fe_4S_4$: Schunn, R. A.; Fritchie, Jr., C. J.; Prewitt, C. T. *Inorg. Chem.* **1966**, *5*, 892. Wei, C. H.; Wilkes, G. R.; Treichel, P. M.; Dahl, L. F. *Inorg. Chem.* **1966**, *5*, 900. $(C_5H_5)_4Co_4S_4$: Uchtman, V.; Dahl, L. F. *J. Am. Chem. Soc.* **1969**, *91*, 3756.

(25) $(C_5R_5)_4Mo_4S_4$: Williams, P. D.; Curtis, M. D.; Duffy, D. N.; Butler, W. M. *Organometallics* **1983**, *2*, 165. Bandy, J. A.; Davies, C. E.; Green, J. C.; Green, M. L. H.; Prout, K.; Rodgers, D. P. S. *J. Chem. Soc., Chem. Commun.* **1983**, 1395. $(i\text{-}PrC_5H_4)_4Mo_4Se_4$ and $(RC_5H_4)_4Cr_4Se_4$: Green, M. L. H.; Hammett, A.; Qin, J.; Baird, P.; Bandy, J. A.; Prout, K.; Marseglia, E.; Obertelli, S. D. *J. Chem. Soc., Chem. Commun.* **1987**, 1811.

(26) $(C_5Me_5)_4Rh_4S_4$: Skaugset, A. E.; Rauchfuss, T. B.; Wilson, S. R. *Organometallics* **1990**, *9*, 2875. Dobbs, D. A.; Bergman, R. G. *J. Am. Chem. Soc.* **1992**, *114*, 6908. Venturelli, A.; Lockemeyer, J. R.; Rauchfuss, T. B. Unpublished results. $(C_5Me_5)_4Rh_4Se_4$: Brunner, H.; Janietz, N.; Wachter, J.; Neumann, H.-P.; Nuber, B.; Ziegler, M. L. *J. Organomet. Chem.* **1990**, *388*, 203.

(27) Wells, A. F. *Structural Inorganic Chemistry*, 5th ed.; Oxford: New York, 1986.

Scheme II

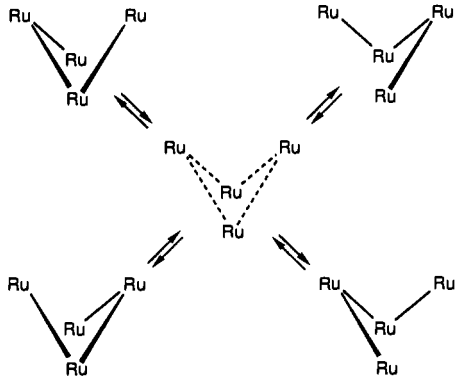

to the formation and cleavage of a M–M bond.[18] The redox-induced bond-forming process represents a balance of several forces including the unfavorable effects of strain (distortion of the neutral precursor) and Coulombic repulsions, counterbalanced by the stabilization associated with the formation of a new M–M bond.

The coalescence of the two methyl signals in the ^{1}H NMR spectra of $(MeC_5H_4)_4Ru_4E_4^{2+}$ provides no insights into the mechanism of the movement of Ru–Ru bonds. The nonequivalence of eight MeC_5H_4 signals (ABCD) in the low-temperature spectra is also consistent with the ground-state structure, which has idealized C_2 symmetry. The ABCD patterns for the two types of (MeC_5H_4)Ru sites reflect the low site symmetries which differ in the number of Ru–Ru bonds. A conceptually simple, but we think unlikely, mechanism for equivalencing the four Ru sites involves a fully delocalized intermediate of idealized T_d symmetry. This mechanism requires rather large structural changes for the three nonbonding Ru···Ru vectors. A D_{2d} intermediate with four delocalized bonding interactions also possesses the correct symmetry properties and is appealing since the nominally isoelectronic cluster $(C_5H_5)_4Fe_4S_4^{2+}$ adopts this structure[20] (Scheme II). In this scenario the dynamics of the cubane dication would involve conversion to a partially delocalized transition state wherein each metal achieves the same fractional oxidation state.

Simpler mechanisms for M–M bond dynamics can be envisioned whereby only one Ru–Ru bond migrates. Such one-bond processes which convert the cluster core to equivalent geometries are summarized in Chart II, where we employ the labels Ru_t and Ru_m for the metals situated at the termini or the middle of the metal–metal bonded Ru–Ru–Ru–Ru sequence. The two types of Ru–Ru bonds are labeled A (there are two of these) and B. Focusing first on migrations of bond B, we see that there are two pathways, B_I and B_{II}, by virtue of the fact that there are two types of Ru···Ru nonbonding edges. The process B_I involves the interchange (TMMT) → (MTTM) and is associated with formal oxidation state changes at all metals since Ru_m sites are Ru^{IV} and Ru_t sites are Ru^{III}. The last column in Chart II depicts the transition state for the process B_I, which is of D_2 symmetry. As such this process does not racemize the cluster. Consequently if this were the only process at work, one would expect to observe a ^{1}H NMR spectrum under fast-exchange conditions consisting of a single Me signal and an ABCD pattern for MeC_5H_4. This clearly is not the case (see Figure 5) since at high temperatures we observe only two MeC_5H_4 signals. It is unlikely that this simple subspectrum arises from accidental degeneracy since the lower temperature ^{1}H NMR spectrum of $(MeC_5H_4)_4Ru_4S_4^{2+}$ shows the eight MeC_5H_4 chemical shifts dispersed over a range of 0.8 ppm. Pathway B_{II} involves a transition state with three Ru···Ru bonding interactions direct at one Ru center. Turning to the processes involving migration of bond A, we see that only pathway A_I results in degenerate site exchange. This "windshield-wiper" like process proceeds via a C_s transition state which

Chart II

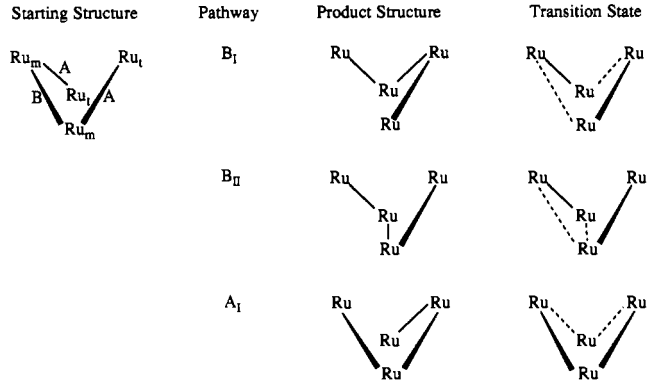

interchanges one Ru_m and one Ru_t site. Ongoing DNMR studies with derivatives of $(MeC_5H_4)_4Ru_4S_4^{2+}$ appear to support this localized mechanism.[28]

Summarizing, a family of mixed-valence Ru_4 clusters are described which are stereochemically nonrigid by virtue of mobile metal–metal bonds. Such structural dynamics are unusual since they are not coupled to other changes in metal ligation. We are currently investigating other clusters that display related structural dynamics.

Experimental Section

Experimental protocols followed those described in previous papers.[14] The Toepler pump was purchased from Pope Scientific (Menomonee Falls, WI). Methylcyclopentadiene was obtained by thermal cracking its dimer at 210 °C followed by fractional distillation at 65 °C. PPh_4Br, NH_4PF_6, and $(MeC_5H_4)_2Fe$ were obtained from Aldrich. Gray selenium (325 mesh) and tellurium powder (100 mesh) were obtained from Alfa. $(MeC_5H_4)Ru(PPh_3)_2X$ (X = Cl, SH, SeH),[14] $RuCl_2(PPh_3)_3$,[29] and $Me_3SiC_5H_5$[30] were prepared by literature methods. Mass spectral data for molecular ions (M^+) and fragments ($M^+ - X$) are calculated using ^{32}S, ^{79}Se, ^{102}Ru, ^{125}Te. FAB-MS employed 3-nitrobenzyl alcohol as a matrix.

Variable-Temperature NMR Studies. Typically 15 mg of the PF_6^- salt was dissolved in ~0.8 mL of CD_3CN (99.96+% *d*, Aldrich) which had been dried over 4-Å sieves. In the case of the $Me_3SiC_5H_4$ compound we employed acetone-d_6. These experiments were performed on a 500-MHz General Electric GN-500 NMR spectrometer with a Doric Trendicator 410A temperature controller (calibrated with MeOH and ethylene glycol standards). Spectra were recorded with 32 pulses and 64 000 data points, a 1-s delay time, and 0.2-Hz line broadening. The –43 °C COSY spectrum of $(MeC_5H_4)_4Ru_4S_4(PF_6)_2$ was collected with a 2-s delay time and a 31-μs pulse width. We estimate that the errors in our values for ΔG^* are <2 kJ/mol; this assumes a combined error in temperatures (T_c and T_{meas}) of ±3 °C and an error of ±5 Hz in $\Delta\nu$.

The exchange of the two Me sites in $(MeC_5H_4)_4Ru_4E_4(PF_6)_2$ (E = S, Se) was evaluated by simulation of ^{1}H NMR spectra (Me region) at nine temperatures for each cluster using the computer program DNMR (Quantum Chemistry Program Exchange, Bloomington, IN). The fits were made by visual matching calculated and observed spectra. The errors in the activation parameters were calculated by the method of Girolami et al.[31]

$(MeC_5H_4)_4Ru_4S_4$. A solution of 1.0 g (1.35 mmol) of $(MeC_5H_4)Ru(PPh_3)_2SH$ in 40 mL of toluene was heated at reflux for 18 h. The resulting red solution was cooled to room temperature and diluted with hexanes to induce crystallization. After several hours at 0 °C, the dark brown needles were collected and washed with hexanes. Yield: 0.20 g (70%). Anal. Calcd for $C_{24}H_{28}Ru_4S_4$: C, 33.96; H, 3.30; S, 15.09. Found: C, 33.97; H, 3.33; S, 14.99. ^{1}H NMR (C_6D_6, 25 °C): δ 4.57 (m, 2H, MeC_5H_4), 4.40 (m, 2H, MeC_5H_4), 1.79 (s, 3H, $CH_3C_5H_4$). EIMS (*m/z*): 852 (M^+), 773 ($M^+ - MeC_5H_4$), 694 ($M^+ - 2MeC_5H_4$), 615 ($M^+ - 3MeC_5H_4$), 536 ($M^+ - 4MeC_5H_4$).

(28) Houser, E. J.; Rauchfuss, T. B.; Wilson, S. R. Unpublished results.
(29) Hallman, P. S.; Stephenson, T. A.; Wilkinson, G. *Inorg. Synth.* **1970**, *12*, 237.
(30) Abel, E. W.; Dunsten, M. O. *J. Organomet. Chem.* **1971**, *33*, 161.
(31) Girolami, G. S. Manuscript in preparation.

Quantitation of H_2 Evolution from Thermolysis of $(MeC_5H_4)Ru(PPh_3)_2SH$. A slurry of 1.0 g (1.36 mmol) of $(MeC_5H_4)Ru(PPh_3)_2SH$ in 100 mL of 1,3,5-trimethylbenzene was prepared in a 500-mL Schlenk tube which was attached to a high-vacuum line. The flask was degassed by freezing (77 K), evacuating (10^{-5} mmHg), and thawing. After several such treatments, the sealed reaction flask was heated to 140 °C with stirring for 12 h. The cooled reaction solution was frozen with liquid nitrogen, and the gases were collected using a Toepler pump. The yield of hydrogen was 4×10^{-4} mol (60%), as identified by EI mass spectrometry. The mesitylene solution was evaporated *in vacuo*, and the solid products were identified as PPh_3 and $(MeC_5H_4)_4Ru_4S_4$. Yield of $(MeC_5H_4)_4Ru_4S_4$: 0.235 g (82%).

$(MeC_5H_4)_4Ru_4Se_4$. A solution of 1.0 g (1.28 mmol) of $(MeC_5H_4)Ru(PPh_3)_2SeH$ in 40 mL of toluene was refluxed for 18 h, during which time the color changed from orange-brown to dark brown. The solution was cooled to room temperature, and 60 mL hexanes were added. After storage at −10 °C for several hours, the dark brown crystals were filtered and washed with hexanes. Yield: 0.20 g (66%). Anal. Calcd for $C_{24}H_{28}Ru_4Se_4$: C, 27.81; H, 2.72; Se, 30.47. Found: C, 27.99; H, 2.79; Se, 30.12. ^{1}H NMR (C_6D_6, 25 °C): δ 4.56 (m, 2H, MeC_5H_4), 4.26 (m, 2H, $Me_3C_5H_4$), 1.87 (s, 3H, $CH_3C_5H_4$). ^{77}Se NMR (C_6D_6, vs external Me_2Se): δ 27.2 ppm.

$(Ph_4P)TeH$. A 3-necked round-bottom flask was fitted with a dry-ice condensor and charged with a glass-coated stir bar, 0.13 g of Na (5.76 mmol), and 100 mL of anhydrous ammonia. This blue solution was treated with 0.37 g of Te (2.88 mmol) powder with stirring. After ca. 1 h the solution was allowed to evaporate and the colorless residue was extracted with 30 mL of deaerated H_2O. The resulting colorless solution was stirred vigorously while being treated dropwise with 28 mL of deaerated 0.1 M HCl (28 mmol) over the course of 20 min to give a pale orange solution. The addition of 1.21 g of Ph_4PBr (2.88 mmol) gave an orange precipitate. The orange powder was filtered out and recrystallized by dissolution in ca. 80 mL of MeOH followed by slow dilution with ca. 120 mL of degassed H_2O to give orange crystals. Yield: 0.98 g (73%). Anal. Calcd for $C_{24}H_{21}PTe$: C, 61.59; H, 4.52; P, 6.62; Te, 27.26. Found: C, 61.49; H, 4.58; P, 6.56; Te, 27.02. ^{1}H NMR (CD_3CN): δ 7.5–8.0 (m, 20H), −13.4 (s, 1H).

$(MeC_5H_4)_4Ru_4Te_4$. To a solution of 0.50 g (1.07 mmol) of $(Ph_4P)TeH$ in 30 mL of MeOH was added 0.5 g (0.67 mmol) of $(MeC_5H_4)Ru(PPh_3)_2Cl$, and the resulting suspension was stirred for 8 h at room temperature. The beige precipitate was collected by filtration and was washed with two 20-mL portions of MeOH. The solid was extracted into 40 mL of toluene, and this solution was heated at reflux for 18 h. The cooled toluene solution was filtered and evaporated to give a black solid, which was washed with hexanes. Recrystallization of the crude solid from 20 mL of CH_2Cl_2 by addition of 50 mL of hexanes gave black crystals of $(MeC_5H_4)_4Ru_4Te_4$. Yield: 0.124 g (60%). Anal. Calcd for $C_{24}H_{28}Ru_4Te_4$: C, 23.41; H, 2.29. Found: C, 23.69; H, 2.44. ^{1}H NMR (C_6D_6): δ 4.66 ppm (s, 2H, MeC_5H_4), 4.28 (s, 2H, MeC_5H_4), 2.06 (s, 3H, $CH_3C_5H_4$). ^{125}Te NMR (C_6D_6, vs external Me_2Te): δ −32.7 (s). FABMS (*m/z*): 1244 (M^+), 1165 ($M^+ - MeC_5H_4$).

$(Me_3SiC_5H_4)Ru(PPh_3)_2Cl$. A solution of 2.8 mL of $Me_3SiC_5H_5$ in 30 mL of THF was heated with 0.16 g of Na wire. After the sodium had completely dissolved (~12 h) the pale pink solution was treated with 6.92 g (7.22 mmol) of $RuCl_2(PPh_3)_3$. The resulting brown solution was then heated to reflux for 6 h giving an orange-red solution. Solvent was removed *in vacuo* leaving a pale yellow solid, which was recrystallized from 20 mL of CH_2Cl_2 by addition of ~80 mL of EtOH. Yield: 4.51 g (79%). Anal. Calcd: C, 66.28; H, 5.31. Found: C, 66.86; H, 5.50. ^{1}H NMR (C_6D_6): δ 7.8 (m, 12 H, $P(C_6H_5)_3$), 6.9 (m, 18 H, $P(C_6H_5)_3$), 4.14 (m, 2 H, $Me_3SiC_5H_4$), 3.72 (m, 2 H, $Me_3SiC_5H_4$), 0.58 ppm (s, 9 H, $(CH_3)_3SiC_5H_4$).

$(Me_3SiC_5H_4)_4Ru_4S_4$. A mixture of 3.10 g (3.89 mmol) of $(Me_3SiC_5H_4)Ru(PPh_3)_2Cl$ and 1.0 g (3.89 mmol) of AgO_3SCF_3 was slurried in 25 mL of CH_2Cl_2 for 4 h and then filtered. The solvent was removed from the filtrate *in vacuo*, and the resulting orange solid was extracted into 20 mL of MeOH. This extract was then added to a solution of 0.33 g (5.89 mmol) of NaSH in 20 mL of MeOH, resulting in the formation of a yellow brown precipitate. This slurry was stirred for 1 h and then filtered, washing the solid with MeOH. A solution of this solid in 30 mL of toluene was heated at reflux for 17 h. The resulting red solution was cooled to room temperature and evaporated to a thick red oil, which was purified by repeated recrystallizations from 10 mL of CH_3CN by addition of 40 mL of EtOH. Yield: 253 mg (24%) based on $(Me_3SiC_5H_4)Ru(PPh_3)_2Cl$). Anal. Calcd for $C_{32}H_{52}Ru_4S_4$: C, 35.53; H, 4.77. Found: C, 35.01; H, 4.77. ^{1}H NMR (C_6D_6): 4.83 (s, 2H, $Me_3SiC_5H_4$), 3.96 (s, 2H, $Me_3SiC_5H_4$), 0.59 (s, 9H, $(CH_3)_3SiC_5H_4$).

$(MeC_5H_4)_2FePF_6$. A 1-L Erlenmeyer flask was charged with 5.06 g (23.6 mmol) of $(MeC_5H_4)_2Fe$ and 50 mL of H_2SO_4. The mixture was stirred for 30 min giving a dark blue solution, which was diluted to ~600 mL with ice water and then filtered. The blue filtrate was treated with 8.0 g (49.1 mmol) of NH_4PF_6 giving a light blue precipitate which was collected by filtration and washed with deionized water. The solid was recrystallized from 70 mL of acetone by addition of 150 mL of hexanes. Yield: 6.84 g (81%). Anal. Calcd for $C_{12}H_{14}F_6FeP$: C, 40.14; H, 3.93. Found: C, 40.45; H, 3.90.

$(MeC_5H_4)_4Ru_4S_4(PF_6)_2$. A 250-mL Schlenk flask was charged with 0.40 g (0.471 mmol) of $(MeC_5H_4)_4Ru_4S_4$, 0.301 g (0.937 mmol) of $(MeC_5H_4)_2FePF_6$ and 30 mL of THF. The solution was stirred for 6 h and filtered leaving a dark brown solid which was recrystallized by dissolution in 20 mL of acetone followed by addition of 80 mL of hexanes. Yield: 0.41 g (76%). Anal. Calcd for $C_{24}H_{28}F_{12}P_2Ru_4S_4$: C, 25.31; H, 2.48. Found: C, 25.66; H, 2.59. ^{1}H NMR (CD_3CN, 20 °C): δ 2.07 (s, 3H, $CH_3C_5H_4$), 5.32 (s, 2H, $CH_3C_5H_4$), 5.57 (s, 2H, $CH_3C_5H_4$). ^{1}H NMR (CD_3CN, −43 °C): δ 1.87 (s, 3H, $CH_3C_5H_4$), 2.10 (s, 3H, $CH_3C_5H_4$), 4.86 (s, 1 H, MeC_5H_4), 5.15 (s, 1 H, MeC_5H_4), 5.17 (s, 1 H, MeC_5H_4), 5.42 (s, 1 H, MeC_5H_4), 5.48 (s, 1 H, MeC_5H_4), 5.63 (s, 1 H, MeC_5H_4), 5.70 (s, 1 H, MeC_5H_4), 5.74 (s, 1 H, MeC_5H_4). $^{13}C\{^1H\}$ NMR (CD_3CN, 20 °C): δ 13.78 (s, $CH_3C_5H_4$), 89.8 (broad s, MeC_5H_4). FABMS (*m/z*): 852 (P^+), 773 ($M^+ - MeC_5H_4$).

$(MeC_5H_4)_4Ru_4Se_4(PF_6)_2$. A 250-mL Schlenk flask was charged with 0.073 g (0.070 mmol) of $(MeC_5H_4)_4Ru_4Se_4$, 0.046 g (0.141 mmol) of $(MeC_5H_4)_2FePF_6$, and 20 mL of THF. The solution was stirred for 3 h and filtered leaving a dark brown solid, which was recrystallized by dissolution in 10 mL of acetone followed by addition of 50 mL of hexanes. Yield: 0.080 g (86%). Anal. Calcd for $C_{24}H_{28}F_{12}P_2Ru_4Se_4$: C, 21.73; H, 2.13. Found: C, 21.82; H, 2.13. ^{1}H NMR (CD_3CN, 20 °C): δ 2.08 (s, 3H, $CH_3C_5H_4$), 5.19 (s, 2H, MeC_5H_4), 5.43 (s, 2H, MeC_5H_4). ^{1}H NMR (CD_3CN, −43 °C): δ 2.00 (s, 3H, $CH_3C_5H_4$), 2.07 (s, 3H, $CH_3C_5H_4$), 4.81 (s, 1 H, MeC_5H_4), 5.04 (s, 1 H, MeC_5H_4), 5.20 (s, 2 H, MeC_5H_4), 5.42 (s 2 H, MeC_5H_4), 5.45 (s, 1 H, MeC_5H_4), 5.58 (s, 1 H, MeC_5H_4). FABMS (*m/z*): 1040 (M^+), 961 ($M^+ - MeC_5H_4$).

$(MeC_5H_4)_4Ru_4Te_4(PF_6)_2$. A 100-mL Schlenk flask was charged with 0.10 g (0.0812 mmol) of $(MeC_5H_4)_4Ru_4Te_4$, 0.0587 g (0.1626 mmol) of $(MeC_5H_4)_2FePF_6$, and 30 mL of THF. The solution was stirred for 7 h and filtered leaving a brown solid which was recrystallized by dissolution in 3 mL of CH_3CN followed by addition of 20 mL of diethyl ether. Yield: 0.10 g (81%). Anal. Calcd for $C_{24}H_{28}F_{12}P_2Ru_4Te_4$: C, 18.95; H, 1.86. Found: C, 19.09; H, 1.91. ^{1}H NMR (CD_3CN, 20 °C): 2.13 (s, 3H), 4.99 (s, 2H), 5.35 (s, 2H). FABMS (*m/z*): 1244 (M^+), 1165 ($M^+ - MeC_5H_4$).

$(Me_3SiC_5H_4)_4Ru_4S_4(PF_6)_2$. A 100-mL Schlenk flask was charged with 0.10 g (0.092 mmol) of $(Me_3SiC_5H_4)_4Ru_4S_4$, 0.067 g (0.184 mmol) of $(MeC_5H_4)_2FePF_6$, and 20 mL of THF. The solution was stirred for 1 h resulting in a color change from blue to orange red. The solvent was removed in vacuo leaving a brown solid which was washed with hexanes and recrystallized from CH_2Cl_2 by the addition of hexanes. Yield: 0.091 g (72%). Anal. Calcd for $C_{32}H_{52}F_{12}P_2Ru_4S_4Si_4$: C, 28.02; H, 3.82. Found: C, 28.07; H, 3.86. ^{1}H NMR (acetone-d_6, 40 °C): δ 0.51 (s, 9H, $(CH_3)_3SiC_5H_4$), 5.41 (broad s, 2H, $Me_3SiC_5H_4$), 6.18 (broad s, 2H, $Me_3SiC_5H_4$). ^{1}H NMR (acetone-d_6, −70 °C): δ 0.40 (s, 9H, $(CH_3)_3SiC_5H_4$), 0.45 (s, 9H, $(CH_3)_3SiC_5H_4$), 4.79 (s, 1H, $Me_3SiC_5H_4$), 4.91 (s, 1H, $Me_3SiC_5H_4$), 5.74 (s, 1H, $Me_3SiC_5H_4$), 5.84 (s, 1H, $Me_3SiC_5H_4$), 5.89 (s, 1H, $Me_3SiC_5H_4$), 5.92 (s, 1H, $Me_3SiC_5H_4$), 6.04 (s, 1H, $Me_3SiC_5H_4$), 6.89 (s, 1H, $Me_3SiC_5H_4$).

$(MeC_5H_4)_4Fe_4S_4(PF_6)_2$. A 100-mL Schlenk flask was charged with 0.20 g (0.299 mmol) of $(MeC_5H_4)_4Fe_4S_4$, 0.215 g (0.60 mmol) of $(MeC_5H_4)_2FePF_6$, and 30 mL of THF. The solution was stirred for 1 h and filtered leaving a brown solid which was twice recrystallized by dissolution in 10 mL of acetone followed by addition of 40 mL of hexanes. Yield: 0.20 g (70%). Anal. Calcd for $C_{24}H_{28}F_{12}Fe_4P_2S_4$: C, 30.09; H, 2.95. Found: C, 30.21; H, 3.08. ^{1}H NMR (CD_3CN): δ 2.08 (s, 3H, $CH_3C_5H_4$), 4.58 (s, 2H, MeC_5H_4), 4.88 (s, 2H, MeC_5H_4).

X-ray Crystallography of $(MeC_5H_4)_4Ru_4Te_4$. Crystals suitable for the X-ray diffraction study were grown by slow evaporation of a CH_2Cl_2 solution of $(MeC_5H_4)_4Ru_4Te_4$. The dark, opaque, columnar crystal used for data collection was $0.04 \times 0.08 \times 0.18$ mm in dimensions. The crystal was approximately bound by the following inversion related forms: $\{1\bar{1}0\}$, $\{110\}$, and $\{11\bar{1}\}$. The crystal was mounted using epoxy to a thin glass fiber with the $\{11\bar{6}\}$ scattering planes roughly normal to the spindle axis.

Table V. Crystal and Data Collection Parameters for $(MeC_5H_4)_4Ru_4Te_4$ and $(Me_3SiC_5H_4)_4Ru_4S_4(PF_6)_2$

formula	$C_{24}H_{28}Ru_4Te_4$	$C_{32}H_{52}F_{12}P_2Ru_4S_4Si_4$
lattice type	monoclinic	monoclinic
space group	$C2/c$	$P2_1/c$
a (Å)	11.943(6)	18.828(2)
b (Å)	18.623(6)	12.421(1)
c (Å)	12.590(7)	21.451(2)
$\alpha = \gamma$ (deg)	90	90
β (deg)	94.32(5)	92.443(1)
V (Å^3)	2792(4)	5012(1)
Z	4	4
d_{calcd} (g/cm^3)	2.929	1.818
μ (cm^{-1})	62.09	15.46
2θ range (deg)	2–50 (for $\pm h,+k,-l$)	3–46 (for $+h,+k,\pm l$)
radiation (λ (Å))	Mo Kα (0.710 73)	Mo Kα (0.710 73)
diffractometer	Enraf-Nonius CAD4 automated K-axis	Syntex $P2_1$ four-circle equipped with Crystal Logic automation
no. of reflcns	2702	7846
no. of unique reflcns	2444	6230
no. of obsd reflcns ($I > 2.58\sigma(I)$)	1136	5204
R_{int}	0.024	0.065
R	0.057	0.050
R_w	0.069	0.070
T_{max}, T_{min}	0.801, 0.592	0.740, 0.614
final diff Fourier	$+1.68 > e/Å^3 > -1.40$	$+1.18 > e/Å^3 > -1.15$

Preliminary photographs and systematic conditions suggested space group Cc or $C2/c$; the centric choice was confirmed by refinement.

The structure was solved by direct methods (SHELXS-86); correct tellurium and ruthenium atom positions were determined from an E-map.[23] Subsequent least-squares refinement and difference Fourier syntheses (SHELX-76) revealed positions for the remaining carbon atoms. The disordered Ru2 cyclopentadienyl ring was constrained to "idealized" geometry; the relative site occupancy for position "A" converged at 0.66(1). Hydrogen atoms were included as fixed contributors in "idealized" positions. Common isotropic thermal parameters were varied for hydrogen and disordered methyl carbon atoms; anisotropic thermal coefficients were refined for the remaining non-hydrogen atoms. Successful convergence was indicated by the maximum shift/error for the last cycle. The highest peaks in the final difference Fourier map were in the vicinity of the four unique heavy atoms. A final analysis of variance between observed and calculated structure factors showed no apparent systematic errors. Intermolecular contacts between disordered methyl hydrogen atoms on adjacent clusters indicate that the scheme used to calculate those positions was not entirely reliable; however, it may also suggest the reason for this disorder. Crystal data collection and refinement parameters are listed in Table V. The unit cell for the cluster is shown in Figure 6.

X-ray Crystallography of $(Me_3SiC_5H_4)_4Ru_4S_4(PF_6)_2$. Crystals suitable for X-ray diffraction study were grown by slow diffusion of hexanes into an acetone solution of $(Me_3SiC_5H_4)_4Ru_4S_4(PF_6)_2$ at 20 °C. The black, opaque, prismatic crystal used for data collection had well-developed faces. There were no crystallites of other contaminating substances attached to the surface of the sample. The crystal was mounted using epoxy to a thin glass fiber with $(01\bar{2})$ scattering planes roughly normal to the spindle axis. The data crystal was approximately bound by the $\{1\bar{2}0\}$ and $\{1\bar{1}0\}$ inversion forms and the $(\bar{1}\bar{2}0)$, (111), and $(31\bar{3})$ faces. Distances from the crystal center to these facial boundaries were 0.14, 0.14, 0.12, 0.12, and 0.15 mm, respectively. No problems were encountered during data collection, and there was no change in the appearance of the sample during the experiment.

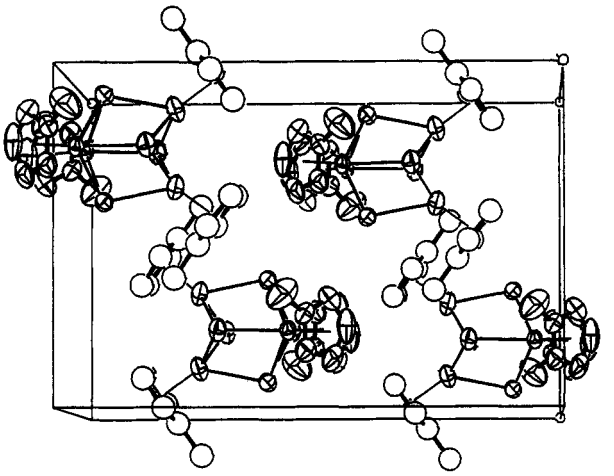

Figure 6. Unit cell of $(MeC_5H_4)_4Ru_4Te_4$.

The structure was solved by direct methods (SHELXS-86); correct ruthenium and sulfur atom positions were deduced from an E-map. Subsequent least-squares refinements and difference Fourier syntheses revealed positions for the remaining non-hydrogen atoms. The hydrogen atoms were included as fixed contributors in "idealized" positions. Both independent anions were disordered in at least two positions: octahedral geometry was imposed on each disordered group. In the final cycle of least-squares refinement, common isotropic parameters were refined for P, F, and H atoms, a common P–F bond length was refined, site occupancy factors were refined for the two disordered anions, and the remaining atoms were independently refined with anisotropic thermal coefficients. Successful convergence was indicated by the maximum shift/error for the last cycle. The highest peaks in the final difference Fourier map were in the vicinity of the disordered anions; the final map had no other significant features. A final analysis of variance between observed and calculated structure factors showed a slight dependence on $\sin(\theta)$. Crystal data collection and refinement parameters are listed in Table V.

Acknowledgment. This research was supported by the National Science Foundation. We thank Professor Gregory S. Girolami for advice on the DNMR measurements.

Supplementary Material Available: Tables of constrained and calculated atomic positions, thermal parameters, and distances and angles (5 pages). Ordering information is given on any current masthead page.